REPORT DOCUMENTATION PAGE

Form Approved OMB No. 0704-0188

1. REPORT DATE *(DD-MM-YYYY)*	2. REPORT TYPE	3. DATES COVERED *(From – To)*
01-08-2006	Final Report	1 June 2005 - 01-Mar-06

4. TITLE AND SUBTITLE

Rare-Earth Oxide Ion (Tm3+, Ho3+, And U3+) Doped Glasses And Fibres For 1.8 To 4 Micrometer Coherent And Broadband Sources

5a. CONTRACT NUMBER
FA8655-05-1-3039

5b. GRANT NUMBER

5c. PROGRAM ELEMENT NUMBER

6. AUTHOR(S)

Professor Animesh Jha

5d. PROJECT NUMBER

5d. TASK NUMBER

5e. WORK UNIT NUMBER

7. PERFORMING ORGANIZATION NAME(S) AND ADDRESS(ES)

University of Leeds
Clarendon Road
Leeds LS2 9JT
United Kingdom

8. PERFORMING ORGANIZATION REPORT NUMBER

N/A

9. SPONSORING/MONITORING AGENCY NAME(S) AND ADDRESS(ES)

EOARD
PSC 821 BOX 14
FPO AE 09421-0014

10. SPONSOR/MONITOR'S ACRONYM(S)

11. SPONSOR/MONITOR'S REPORT NUMBER(S)
Grant 05-3039

12. DISTRIBUTION/AVAILABILITY STATEMENT

Approved for public release; distribution is unlimited.

13. SUPPLEMENTARY NOTES

14. ABSTRACT

This report results from a contract tasking University of Leeds as follows: Task 1: (0 - 5 months): Optimise tellurium oxide (TeO2) , fluorine-containing silicate (SiOF2) and germanate (GeOF2) glass hosts for each dopant by characterising the spectroscopic properties, including absorption and emission cross-sections and the lifetimes of the lasing levels. Design multimode fibres for the analysis of pump photon ion interaction, and for examining any detrimental effects. A preliminary investigation on various pumping schemes using semiconductor diode laser wavelengths at 800 nm, 940 nm, 960 nm, 980 nm, 1480 and 1550 nm will be explored.
Deliverable Report 1: A comparison of the spectroscopic properties of RE-ion (doped Tm3+, Ho3+, and U3+) and their suitability for tunable laser source.
Task 2 (6 -7th month): Multimode fibres will be drawn to study the interaction of pump photons in a long interaction path length, from which we will be able to investigate the potential sources of ESA, favourable or detrimental energy transfer and pumping scheme. Also consider whether all the dopants should be incorporated in a single core, or to have each dopant in a separate core around a common cladding, so that the high-power pump source can provide sufficient excitation for Tm3+, Ho3+, and U3+ acceptor ions and Yb3+ as the sensitizer ions.
Task 3 (8th - 9th month): Quantify the quantum efficiency of individual transitions in the dopants,. Using carefully designed fibres with Ho or Tm, undertake a preliminary investigation of the laser experiment and establish the required threshold and slope efficiency in either a Tm-doped or Ho-doped fibres.
Deliverable report 2:Summary of fibre spectroscopy and preliminary gain characterisation using a suitable pumping scheme.

15. SUBJECT TERMS

EOARD, Solid state lasers, Crystal Growth

16. SECURITY CLASSIFICATION OF:			17. LIMITATION OF ABSTRACT	18, NUMBER OF PAGES	19a. NAME OF RESPONSIBLE PERSON
a. REPORT	b. ABSTRACT	c. THIS PAGE			DONALD J SMITH
UNCLAS	UNCLAS	UNCLAS	UL	9	19b. TELEPHONE NUMBER *(Include area code)* +44 (0)20 7514 4953

Rare-earth oxide ion (Tm^{3+}, Ho^{3+}, and U^{3+}) doped glasses and fibres for 1.8 to 4 micrometer coherent and broadband sources

Report prepared for EOARD.
FAO: Sandy Smith.

Project No. 053039

Billy Richards, Shaoxiong Shen, Animesh Jha

Institute for Materials Research, Houldsworth Building, University of Leeds, Clarendon Road, Leeds, LS2 9JT

24 July 2006

Deliverable Report 2
A comparison of the spectroscopic properties of RE-ion doped (Tm^{3+}, Ho^{3+}, and Yb^{3+}) glasses and fibres for their suitability for tuneable laser source in mid-IR (1800-2300 nm).

ABSTRACT

The visible and infrared emission spectra of Tm^{3+}, Tm^{3+}-Ho^{3+} and Tm^{3+}-Yb^{3+} doped tellurite fibres have been measured and studied for potential mid-IR fibre laser design. When pumped with an 808 nm source, Tm^{3+} doped fibre shows emission at ~1.46 and ~1.86 μm from the $^3H_4 \rightarrow {}^3F_4$ and $^3F_4 \rightarrow {}^3H_6$ transitions respectively, and co-doping with Ho^{3+} results in emission at ~2.0 μm through energy transfer from the $^3F_4$ Tm^{3+} level to the $^5I_7$ Ho^{3+} level. Yb^{3+} ions act as sensitizers and allow the use of a 978 nm pump source populating the upper laser level of Tm^{3+} through energy transfer. Tellurite fibre offers the advantage that relatively short lengths of fibre can be used to create fibre lasers, which is desirable for compact device fabrication. We have observed lasing action at 1.53 μm in around 10 cm lengths of Er^{3+} doped tellurite fibre. A range of lengths of multi mode and single mode fibre were measured and compared to the bulk glass samples of the same dopant concentrations. The length of these fibres was found to significantly affect the shape and position of the emission peaks, with longer lengths causing narrowing of the peak and shifting to longer wavelengths. The emission spectra of Tm^{3+} doped commercially bought silica fibre was also measured to compare with the tellurite fibre.

INTRODUCTION

Tellurite glass has several properties which make it an interesting candidate for mid-IR fibre laser design and use in other optical devices. The transmission range of tellurium based glasses extends into the mid infra red up to around 5 μm and has a low cut-off phonon energy of around 800cm^{-1}[1]. Both of these properties compare well against other oxide based glasses such as silicates. This feature, coupled with the high rare earth ion solubility, makes tellurium based glass a good host within which to examine the longer wavelength transitions of Tm^{3+} and Ho^{3+} ions. Tellurite glass has a high refractive index which increases the absorption and emission cross-sections [2], good optical and mechanical properties and is relatively easy to manufacture having a low melting point.

Mid-IR fibre lasers in the range 1.8-2.9 μm and beyond have various potential applications including eye-safe laser lidar and remote chemical sensing, including the characterisation of CO_2 and OH which both have very strong absorption bands in the mid-IR. The strong absorption from water in this region makes these compact laser sources attractive for medical surgery applications. There are many reports of Tm^{3+} doped silica fibre lasers operating at around 2 μm [3-7], and of Tm^{3+} and Tm^{3+}/ Ho^{3+}co-doped fluoride based fibre lasers operating in the 1.8 to 2.9 μm region[8-12]. There are however very few reports of tellurite fibre lasers operating in the longer wavelength end of this range. The development of these lasers in tellurite fibre is desirable due to the fact that the glass is much more stable and resistant to corrosion than fluoride glass leading to fewer design and operation problems [13].

The Tm^{3+} ions can be pumped directly into the $^3H_4$ level with an 800 nm source and will show emission at around 1.46 μm ($^3H_4$-$^3F_4$) and 1.8 μm ($^3F_4$-$^3H_6$). Ho^{3+} cannot be pumped directly with an 800 nm source due to the lack of an appropriate absorption band. In a Tm^{3+}- Ho^{3+} co-doped glass, the $^3H_4$ Tm^{3+} level is populated by the 800 nm pump source and a quenching mechanism transfers energy to the $^5I_7$ Ho^{3+} level which then radiatively depopulates to the Ho^{3+} ground state ($^5I_8$) giving rise to emission at around 2.0 μm [14]. Tm^{3+} and Ho^{3+} can also be co-doped with Yb^{3+} which acts as an effective sensitizer. The Yb^{3+} can be pumped with a 980 nm source into the $^2F_{5/2}$ level which can then through energy transfer mechanisms, populate the Tm^{3+} $^3H_5$ and Ho^{3+} $^5I_6$ levels. The absorption band of Yb^{3+} at 980 nm makes it very convenient for use with readily available diode lasers, and because of the Yb^{3+} ion energy level structure there is no possibility of excited state absorption making Yb^{3+} co-doped devices more efficient [15].

This report details the results of the emission spectroscopy of the Tm^{3+}, Ho^{3+} and Yb^{3+} doped tellurite and silica fibre in the infrared and visible regions and uses these results to explain the pumping schemes and energy transfer processes within these rare-earth ion dopants.

EXPERIMENTAL

The tellurite fibres were manufactured from glass with the composition 78TeO_2-12ZnO-10Na_2O (mol%) for the core and 75TeO_2-15ZnO-10Na_2O (mol%) for the cladding. Tm_2O_3 (0.5 wt%) doped, Tm_2O_3-Ho_2O_3 (0.5-1.0 wt%) codoped and Tm_2O_3-Yb_2O_3 (0.5-1.0 wt%) codoped fibres were investigated. The starting chemicals for the core and cladding glasses were weighed, ground, mixed and then placed into gold crucibles and melted in separate electric tube furnaces in a dry O_2 atmosphere. The powders are initially dried overnight and then melted at 820ºC. The mixtures were stirred after 1 hour with a gold rod and then homogenized at 720ºC for 2 hours. The fibre preform is cast using the suction method into a

preheated brass mould and then annealed at 300ºC for 3 hours, after which it is allowed to cool slowly in the furnace to room temperature. The preforms are extruded into structured rods which can then be further extruded with cladding tubes made by the rotation method to reduce the core diameter. Fibre is drawn at each stage providing a range of fibres with varying core diameter. The silica fibre tested was bought from the National Optics Institute, (INO, Canada), and was a 10 m Tm^{3+} doped double-clad fibre with a D-shaped inner cladding and a 20 µm core diameter.

Infrared fluorescence spectra of fibre and bulk glass were measured in the wavelength range 1.3 – 2.2 µm using an Edinburgh Instruments FLS920 Steady State and Time Resolved Fluorescence Spectrometer fitted with an InGaAs detector. Samples were excited either with an 808 nm or 978 nm laser diode source. Lifetime measurements were made by modulating the laser diode current supply with an external function generator and capturing the fluorescence decay using a digital oscilloscope (Tektronics, TDS3012). All experiments were carried out at room temperature.

RESULTS AND DISCUSSIONS

Infrared emission in Tm^{3+} doped tellurite fibre

Figure 1 shows the emission spectra of a range of lengths of multi mode Tm^{3+} doped tellurite fibre with a core diameter of approximately 12 µm when pumped with an 808 nm laser diode source. The doping concentration in this fibre is 0.5 wt%. The spectra have been normalised with respect to the peak at ~1.86 µm which is attributed to $^3F_4 \rightarrow {}^3H_6$ transition of Tm^{3+}. As the length of the fibre increases, the peak shifts to longer wavelengths due to ground-state absorption and re-emission of light within these two energy levels. The figure also compares the fibre emission spectra to that of the bulk glass sample with the same doping concentration. The $^3F_4 \rightarrow {}^3H_6$ peaks measured in the fibre samples are narrower than the bulk glass sample and also shifted to longer wavelengths. In fibre the peak at 1.46 µm due to the $^3H_4 \rightarrow {}^3F_4$ transition is lower in intensity relative to the ~1.86 µm peak than in the bulk sample showing that the confinements of the fibre geometry are increasing the energy transfer efficiency between Tm^{3+} ions. The emission spectra of different lengths of single mode Tm^{3+} doped tellurite fibre were also measured which showed the same trends as for the multi mode fibres.

The measured fluorescence lifetime from the $^3F_4$ Tm^{3+} level was 1633 µs in bulk glass and increased from 1941 µs to 2290 µs in increasing lengths of singly doped multi mode fibre. This increase in lifetime is due to the absorption and re-emission of fluorescence which re-populates the $^3F_4$ level. It has been found that the lifetime value measured can be affected by the signal intensity and width of the pump pulse used. Longer pulse durations result in higher signal intensity and a shorter lifetime value than for short pulses/lower signal intensity. While this effect becomes quite significant for very short lifetime transitions, it is less so for long lifetimes such as the ones studied here. However, the length of the fibre under test affects the signal intensity, and other effects such as energy trapping within the fibre could mean that the measured lifetime is not necessarily the true lifetime. These effects are currently being studied to gain more understanding into the processes involved.

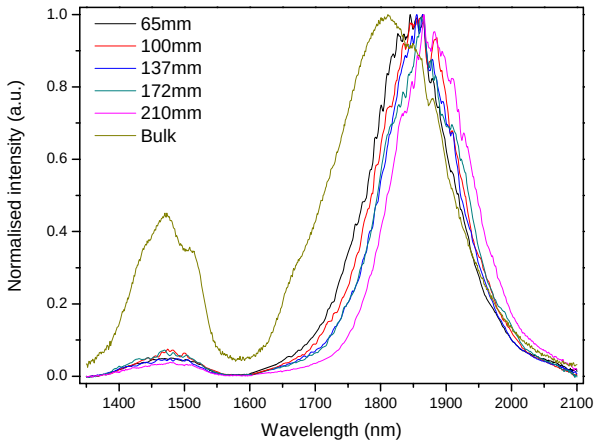

Fig. 1. The emission spectra of 0.5 wt% Tm^{3+} doped tellurite fibre (core diameter = 12µm) and bulk glass when excited with an 808 nm laser source. The spectra have been normalised with respect to the peak at ~1.86 µm.

Infrared emission in Tm^{3+}-Ho^{3+} doped tellurite fibre

Figure 2 shows the emission spectra of varying lengths of 0.5 wt% Tm^{3+} and 1.0 wt% Ho^{3+} codoped tellurite fibre which are compared to the bulk glass sample of the same dopant concentration when excited with the same 808 nm laser source. The fibres are multi mode with a core diameter of approximately 12 µm. The spectra have been normalized with respect to the peak at ~2.0 µm which is attributed to the $^5I_7 \rightarrow {}^5I_8$ Ho^{3+} transition. The spectra show that the shape of the emission peak from this transition is different when measured in fibre or bulk glass. In fibre the peak is narrowed and shifted to longer wavelengths and also appears as a single peak instead of a double peak in bulk glass. Ground state absorption and re-emission in the Ho^{3+} ions due to the increased path length and energy confinement in the fibre results in emission only from the longer wavelength levels in the $^5I_7$ manifold. The peak at 1.46 µm and shoulder at ~1.86 µm are due to the $^3H_4 \rightarrow {}^3F_4$ and $^3F_4 \rightarrow {}^3H_6$ transitions respectively in Tm^{3+}. The intensities of these peaks relative to the ~2.0 µm peak are much lower in fibre than bulk glass. Ho^{3+} ions cannot be directly excited with an 808 nm source which means that energy must be transferred to Ho^{3+} from the Tm^{3+} ions. The reduction in intensity of the Tm^{3+} peaks in figure 3 shows that the energy transfer processes from Tm^{3+} to Ho^{3+} are becoming more efficient in fibre over bulk glass. The intensity of the peak at 1.46 µm increases with fibre length suggesting a back energy transfer process from Ho^{3+} to Tm^{3+} ions due to the upconversion in Ho^{3+} which increases in longer fibres. This also suggests that for operation at ~2.0 µm in this fibre, shorter lengths are preferable. In single mode geometries of this fibre the spectra shape are similar but with smaller 1.46 µm peak intensities confirming that the increased energy confinement in the fibre geometry is increasing the energy transfer from the $^3H_4 \rightarrow {}^3F_4$ Tm^{3+} transition to the $^5I_8 \rightarrow {}^5I_7$ Ho^{3+} transition. The lifetime of the $^5I_7$ Ho^{3+} level in bulk glass is 3148 µs and in multi mode fibre 4200-4500 µs but does not appear to vary with fibre length. The increase in lifetime in fibre over bulk glass further confirms the increased energy transfer to the $^5I_7$ level in the fibre geometry.

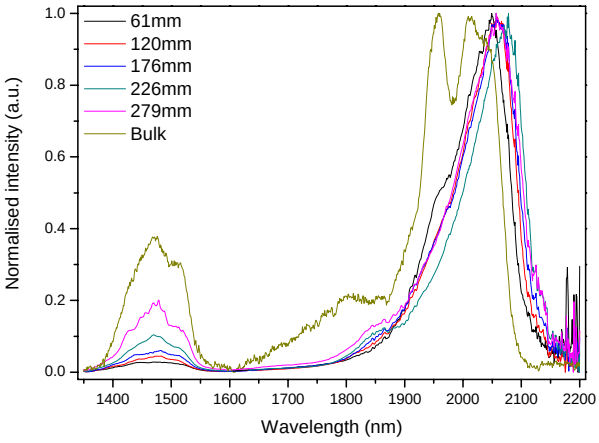

Fig. 2. The emission spectra of 0.5 wt% Tm^{3+}-1.0 wt% Ho^{3+} codoped tellurite fibre (core diameter = 12µm) and bulk glass when excited with an 808 nm laser source. The spectra have been normalized with respect to the peak at ~2.0 µm.

Infrared emission in Tm^{3+}-Yb^{3+} doped tellurite fibre

Figure 3 shows the emission spectra of 0.5 wt% Tm^{3+} and 1.0 wt% Yb^{3+} codoped fibre of varying length with a core diameter of approximately 12 µm. The use of Yb^{3+} as a sensitizer in this fibre allowed the use of a 978 nm pump source to populate the $^3H_5$ level of Tm^{3+} through energy transfer from Yb^{3+}. Yb^{3+} has an absorption peak centred close to 978 nm due to the $^2F_{7/2} \rightarrow {}^2F_{5/2}$ transition which is more intense than the Tm^{3+} absorption peaks making this an efficient pumping scheme [2]. Coupling of this pump source into the fibre was much improved over the 808 nm source due to the single mode nature of the pump diode output. The emission spectra have been normalized with respect to the peak from the $^3F_4 \rightarrow {}^3H_6$ Tm^{3+} transition. The results again show a narrowing and shifting to longer wavelengths with increasing fibre length. The peak at ~1.5 µm is from the $^3H_4 \rightarrow {}^3F_4$ transition of Tm^{3+} which must be caused by upconversion in Tm^{3+} due to the fact that energy transfer from Yb^{3+} populates the lower lying $^3H_5$ level of Tm^{3+}. The intensity of this peak is lower in shorter lengths of fibre and in the single mode geometry. The lifetime of the $^3F_4$ level in this fibre was generally slightly shorter than in the pure Tm^{3+} doped fibre due to the increased upconversion, and did not seem to vary with length.

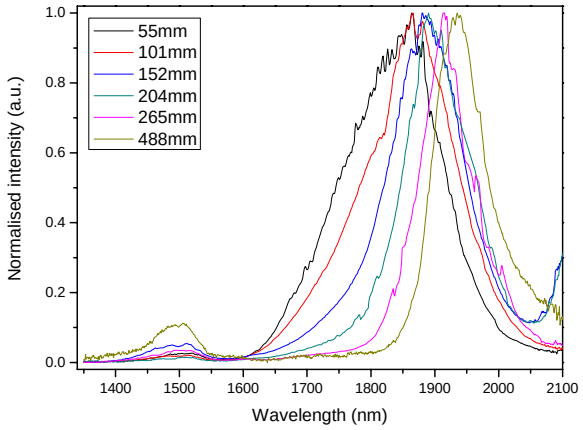

Fig. 3. The emission spectra of 0.5 wt% Tm^{3+}-1.0 wt% Yb^{3+} codoped tellurite fibre (core diameter = 12µm) when excited with an 978 nm laser source. The spectra have been normalized with respect to the peak at ~1.86 µm.

Visible upconversion in Tm^{3+}, Tm^{3+}-Ho^{3+} and Tm^{3+}-Yb^{3+} dope tellurite fibres

Strong visible emission due to upconversion was observed in all these fibres, so to further understand the fluorescence and energy transfer mechanisms, the visible emission spectra were also measured at room temperature using the same pump sources as for the infrared measurements. These results can be found in figure 4 and are all measured using single mode fibre. Graph (a) and (b) do not show the emission at 800 nm from the $^3H_4$ level of Tm^{3+} because a filter had to be used to attenuate the unabsorbed pump light which was saturating the detector. This emission can be seen in graph (c) however as the pump (at 978 nm) was out of the detection range thus not requiring the filter. The Tm^{3+} doped fibre shows weak blue emission at 480 nm due to the $^1G_4 \rightarrow {}^3H_6$ transition arising from a two pump photon excited state absorption (ESA) process. In graph (a) there also appears to be emission at 525 and 550 nm but this is not due to the Tm^{3+} ions. These peaks have been seen in other fibres, (including undoped ones), and is believed to be due to some possible contamination arising during the fibre fabrication process. It is possible that the peak at 550 nm is due to Ho_2O_3 contamination in the Tm_2O_3. The peak is in the same region as would be expected from Ho^{3+} ions and having other rare earth contaminants could be likely due to the difficulty in purifying them due to their similar chemistries. The intensity of the blue emission in the Tm^{3+} doped fibre is extremely low compared to the emission in the other two fibres which is why these contamination peaks are visible in this spectrum but not in the other two. The Tm^{3+}-Ho^{3+} doped fibre shows additional emission at 550 nm which is due to the $(^5S_2, {}^5F_4) \rightarrow {}^5I_8$ Ho^{3+} transition. In this fibre the blue and green emission lines are significantly narrowed which suggests superfluorescence and promise for visible laser operation. The Tm^{3+}-Yb^{3+} codoped fibre shows strong emission at 480 and 650 and 800 nm due to the $^1G_4 \rightarrow {}^3H_6$, $^1G_4 \rightarrow {}^3F_4$ and $^3H_4 \rightarrow {}^3H_6$ Tm^{3+} transitions respectively.

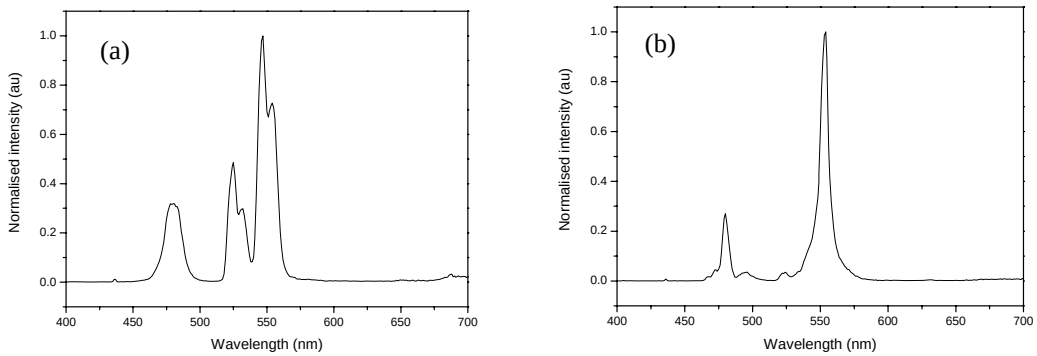

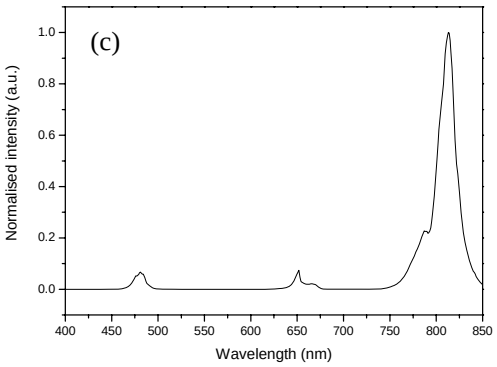

Fig. 4. The visible upconversion emission spectra for (a) 0.5 wt% Tm^{3+} doped tellurite fibre with 808 nm pump (b) 0.5 wt% Tm^{3+} - 1.0 wt% Ho^{3+} codoped tellurite fibre with 808 nm pump and (c) 0.5 wt% Tm^{3+} - 1.0 wt% Yb^{3+} codoped tellurite fibre with 978 nm pump.

Figure 5 shows the energy level diagrams for the three systems studied showing the pumping, energy transfer and upconversion mechanisms. The 808 nm pump excites the $^3H_4$ Tm^{3+} level which decays to the $^3F_4$ level emitting a 1.46 µm photon and then to the $^3H_6$ level emitting the 1.86 µm photon. At high Tm^{3+} concentration and in fibre, a quenching mechanism takes place between Tm^{3+} ions and energy is directly transferred non-radiatively from one ion to another. One ion decays from the $^3H_4$ to the $^3F_4$ while the other ion is excited from the $^3H_6$ ground state to the $^3F_4$ level. This process results in two Tm^{3+} ions being excited to the $^3F_4$ level for one 800 nm pump photon. Stokes energy transfer also occurs from an ion decaying from the $^3F_4$ level exciting another ion to the $^3F_4$ level. ESA excites a Tm^{3+} ion from the $^3H_5$ level to the $^1G_4$ level which decays to the ground state giving rise to the small 480 nm peak in fig 5 (a). This peak is very low in intensity because the upconversion to $^1G_4$ is originating from the $^3H_5$ level which will undergo fast non-radiative decay to $^3F_4$. Upconversion emission has been observed [16] at ~376 nm in Tm^{3+} doped fluoride glass due to the $^1D_2 \rightarrow {}^3H_6$ transition which is not seen in our tellurite glass because the corresponding energy of this transition falls in the UV absorption edge and is therefore quenched.

In the Tm^{3+}-Ho^{3+} fibre the Tm^{3+} ions are pumped in the same way as above and energy is transferred non-radiatively to the Ho^{3+} ions where the Tm^{3+} ion decays from the $^3F_4$ level to the ground state and the Ho^{3+} ion is excited from the $^5I_8$ ground state to the $^5I_7$ level where it decays emitting a 2.05 µm photon. Upconversion excites the Ho^{3+} ion to the $^5I_5$ level which then decays non-radiatively to the $^5I_6$ level, is back transferred to the $^3H_5$ Tm^{3+} level which decays non-radiatively to the $^3F_4$ level where energy is transferred back to the Ho^{3+} $^5I_7$ level emitting a 2.05 µm photon [14]. Upconversion also populates the $^5S_2$ and $^5F_4$ levels of Ho^{3+} which de-excite to the ground state giving rise to the green emission at 550 nm. The addition of the Ho^{3+} ions enhances the upconversion to the $^1G_4$ Tm^{3+} level and consequently the blue emission intensity at 480 nm.

In the Tm^{3+}-Yb^{3+} codoped fibre the 976 nm pump excites the $^2F_{5/2}$ Yb^{3+} level which exhibits fluorescence at 1020 nm pumping the Tm^{3+} ions into the $^3H_5$ level. This level decays non-radiatively to $^3F_4$ and then radiatively to the ground state emitting the 1.86 µm photon. Two photon upconversion populates the $^3H_4$ Tm^{3+} level which decays to the ground state emitting an 800 nm photon and three photon upconversion populates the $^1G_4$ which decays to the $^3F_4$ and $^3H_6$ levels giving strong emission at 650 nm (red) and 480 nm (blue) respectively[17][18].

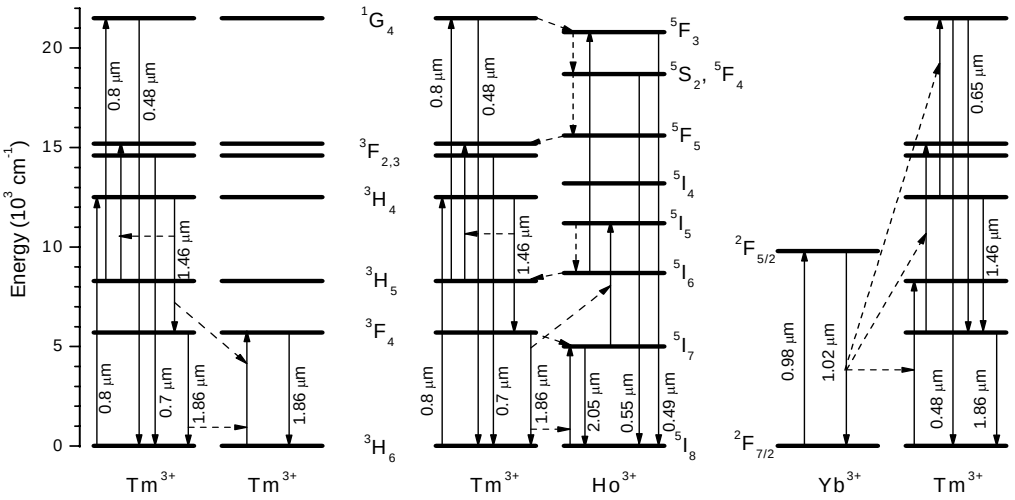

Fig. 5. Energy level diagrams for the Tm^{3+}-Tm^{3+}, Tm^{3+}-Ho^{3+} and Tm^{3+}-Yb^{3+} systems showing the pumping schemes, multiple photon upconversion and energy transfer, (represented by the dashed arrows).

Tm^{3+} doped silica fibre

Figure 6 shows the infrared emission spectrum of the 10 m length of Tm^{3+} doped double clad silica fibre when pumped with around 1.8 W, 808 nm laser source. The graph also shows the spectrum of the 210 mm length of Tm^{3+} doped multi mode tellurite fibre for comparison. The silica fibre has emission peaks at around 1.45 and 1.85 µm which are due to the $^3H_4$-$^3F_4$ and $^3F_4$-$^3H_6$ transitions respectively. Although these peaks are due to the same transitions as in the tellurite fibre, the peak shapes are different due to the change in host glass causing the ratio of transitions from the various Stark levels within the manifolds to change. The spectrum for the tellurite fibre is narrower than the silica fibre and the 1.85 µm peak is shifted to longer wavelengths. This suggests that the emission in the tellurite fibre is starting to superfluoresce. The silica fibre also showed weak emission at 480 nm due to upconversion and emission due to the $^1G_4$-$^3H_6$ transition. Figure 7 shows the decay curve for emission at 1852 nm in the silica fibre when pumped with a modulating 808 nm laser source. The lifetime of the $^3F_4$ level in silica level was measured to be around 650 µs compared to around 2290 µs in the 210 mm length of tellurite fibre. A long upper laser level lifetime is desirable for non-terminating CW laser operation, and these results confirm the potential advantages of tellurite fibre for compact fibre laser sources.

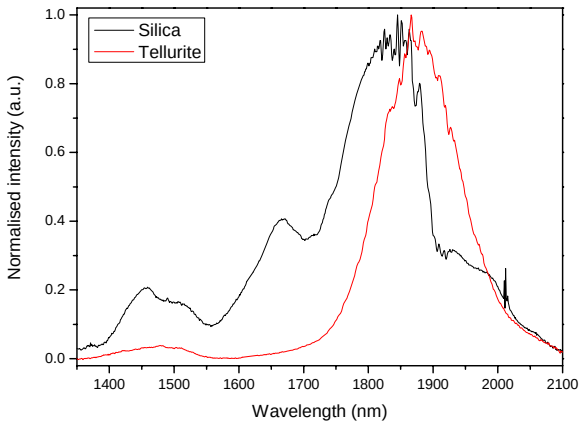

Fig. 6. The emission spectra of Tm^{3+} doped silica and tellurite fibre when excited with an 808 nm laser source. The spectra have been normalized with respect to the peak at ~1.86 µm.

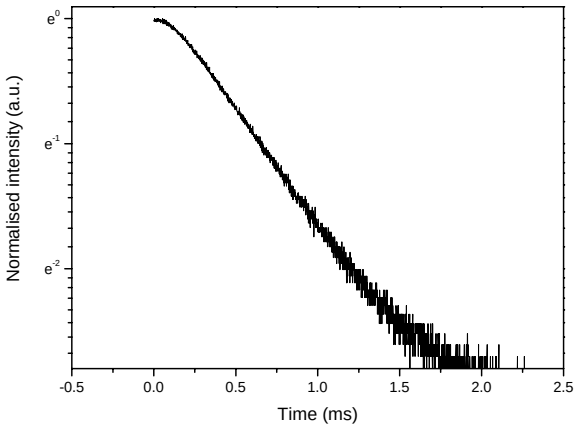

Fig. 7. The emission decay curve at 1852 nm for the Tm^{3+} doped silica fibre when excited with a modulated 808 nm laser source.

CONCLUSION

Mid-IR emission in the 1.8 – 2.1 μm range has been measured in Tm^{3+} doped and Tm^{3+}-Ho^{3+} codoped tellurite fibres when excited with an 808 nm pump. Tm^{3+} doped fibre shows strong emission at ~1.86 μm while the Tm^{3+}-Ho^{3+} codoped fibre shows emission at ~2.05 μm through energy transfer to the Ho^{3+} ions. Emission has also been observed at ~1.86 μm in Tm^{3+}-Yb^{3+} codoped fibre when pumped with a 976 nm source. These measurements show narrowing and red-shifting of emission peaks and increased energy transfer in the smaller geometries associated with these fibres. The visible upconversion emission has been measured and used to help explain the energy transfer processes involved. Emission has also been measured in a 10 m length of Tm^{3+} doped double-clad silica fibre which exhibits a broader peak and a shorter lifetime at ~1.86 μm than in the tellurite fibre. These results suggest that short lengths (<0.5 m) of doped tellurite fibre can be used for mid-IR fibre laser sources.

REFERENCES

[1] L. D. da Vila, L. Gomes, C. R. Eyzaguirre, E. Rodriguez, C. L. Cesar, L. C. Barbosa, Opt. Mater. **27** (2005) 1333-1339.
[2] L. Huang, S. Shen, A. Jha, J. Non-Cryst. Solids **345&346** (2004) 349-353.
[3] Y. H. Tsang, D. J. Coleman, T. A. King, Opt. Comm. **231** (2004) 357-364.
[4] D. C. Hanna, I. R. Perry, J. R. Lincoln, Opt. Comm. Vol. **80**. No. 1. (1990).
[5] B. C. Dickinson, S. D. Jackson, T. A. King, Opt. Comm. **182** (2000) 199-203.
[6] W. A. Clarkson, N. P. Barnes, P. W. Turner, J. Nilsson, D. C. Hanna, Opt. Lett. Vol. **27**. No. 22. (2002).
[7] A. F. El-Sherif, T. A. King, Opt. Lett. Vol. **28**. No. 1. (2003).
[8] J. Y. Allain, M. Monerie, H. Poignant, Electron. Lett. Vol. **25**. No. 24. (1989).
[9] R. G. Smart, J. N. Carter, A. C. Tropper, D. C. Hanna, Opt. Comm. Vol. **82**. No. 5,6. (1991).
[10] M. Doshida, M. Obara, Jpn. J. Appl. Phys. **34** (1995) 6079-6083.
[11] L. Esterowitz, R. Allen, I. Aggarwal, Electron. Lett. Vol. **24**. No. 17. (1988).
[12] S. D. Jackson, Electron. Lett. Vol. **37**. No. 13. (2001).
[13] S. Shen, A. Jha, E. Zhang, S. J. Wilson, C. R. Chimie **5** (2002) 921-938.
[14] X. Zou, H. Toratani, J. Non-Cryst Solids **195** (1996) 113-124.
[15] L. C. Courrol, L. V. G. Tarelho, L. Gomes, N. D. Vieira Jr, F. C. Cassanjes, Y. Messaddeq, S. J. L. Ribeiro, J. Non-Cryst Solids **284** (2001) 217-222.
[16] N. Rakov, G. Maciel, M. Sundheimer, L. Menezes, A. Gomes, Y. Messaddeq, F. Cassanjes, G. Poirier, S. Ribeiro, J. App. Phys. Comm. Vol. **92**, No. 10 (2002) 6337.
[17] S. Shen, A. Jha, L. Huang, P. Joshi, Opt. Lett. Vol. **30**, No. 12, 1437 (2005)
[18] G. Wang, S. Dai, J. Zhang, L. Wen, J. Yang, Z. Jiang, Spectrochim. Acta A **64,** 349 (2005)